275 NO

MSC INTERNAL NOTE 65-EC-11

PROJECT APOLLO

LINEARIZED STATISTICAL ERROR ANALYSIS OF APOLLO LUNAR EXCURSION MODULE ASCENT AND RENDEZVOUS FOR COMPARISON OF SEVERAL MEASUREMENT SCHEMES

Prepared by: R. H. Kidd III
R. H. Kidd, III

T. M. Carney
T. M. Carney

J. H. Suddath
J. H. Suddath

Approved:
Kenneth J. Cox
Chief, Systems Analysis Branch

Approved:
Robert C. Duncan
Chief, Guidance and Control Division

NATIONAL AERONAUTICS AND SPACE ADMINISTRATION
MANNED SPACECRAFT CENTER
HOUSTON, TEXAS
March 12, 1965

SUMMARY

A linearized analysis of the Apollo Lunar Excursion Module ascent and rendezvous operation, including the navigation and guidance, was made to evaluate the comparative performance of several measurement schemes. The statistical dispersions and uncertainties were computed for various initial error covariance matrices and the following navigation measurement schemes; radar, optical tracker, V.H.F. radio range plus sextant and sextant alone. The precision and operating constraints of each of the sensors was based as nearly as possible on specification values.

Results of the investigation are a measure of the corrective velocity increment requirement and the vehicle state deviation and uncertainty in the neighborhood of the docking interface tabulated for each measurement configuration. For nominal specified precision and operation, the overall performance of the optical tracker was best, followed in order by the VHF sextant combination, the sextant alone and the radar.

INTRODUCTION

The study reported is a linearized statistical error analysis of the Apollo Lunar Excursion Module (LEM) ascent phase from launch burnout to the point of pilot takeover for the docking maneuver. This effort was motivated by a Guidance and Control Division investigation of replacements for the rendezvous radar installation on the Apollo Command and Service Module (CSM). Accordingly, the analysis was weighted to simulate the navigation instrument effects well, using reasonable representations for the other elements of the mission.

The primary guidance and navigation configuration during LEM ascent consists of some measuring device to provide information on the relative state of the LEM and CSM, the Kalman filter to process this information to give an estimate of position and velocity, and an explicit guidance scheme based on Lambert's problem to provide midcourse correction capability and, in the terminal phase, to allow the vehicle to follow a desired range/range-rate schedule. For various contingencies, the measurements and estimation can be performed on the CSM rather than the LEM, and the corrections can be performed by either vehicle.

A digital computer program written for the CDC 3600 was used to carry out the study. This program calculates a reference trajectory for both the LEM and the CSM during an ascent from arbitrary initial conditions at shutdown of the LEM ascent engine. The trajectory is carried through midcourse to the terminal rendezvous phase, where velocity corrections are generated and added according to MIT's range/range-rate schedule, up to a relative range of 250 feet. This places the vehicles within the docking range. Along with the reference trajectories, covariance matrices for dispersions from the reference and for uncertainties in estimation of the

vehicle state are extrapolated along the LEM trajectory. Measurements are introduced at a specified rate and are used to reduce the uncertainties by means of the Kalman filter. During the midcourse phase, corrective velocity requirements are calculated by a classical linearization of Lambert's problem and the effect of a correction is applied to the dispersion covariance matrix whenever certain criteria are satisfied. During the terminal phase, a similar linearized guidance technique is used to determine the additional velocity increment required at each nominal correction due to the dispersions.

The results of this program, as presently reported, are an RMS velocity increment for midcourse corrections and for dispersions about the nominal terminal corrections, and the RMS uncertainties and deviations in position and velocity in the docking neighborhood. These quantities provide an effective measure of the relative merits of the various measurement schemes investigated.

The measurement schemes considered were:

a. Radar - measuring azimuth and elevation angles from an inertial reference throughout, range-rate in the midcourse phase and range in the terminal phase.

b. Optical tracker - measuring azimuth and elevation angles from an inertial reference throughout.

c, V.H.F. - Sextant - measuring radio range and azimuth and elevation angles from an inertial reference during the midcourse phase and either all these quantities, range alone, or nothing during the terminal phase.

d. Sextant - measuring azimuth and elevation angles from an inertial reference during the midcourse phase,no measurements in the terminal phase.

A number of different initial dispersion matrices corresponding to various contingencies were used to exercise the above measuring schemes with varying error configurations.

I. TRAJECTORY MODEL

In error analyses of orbital mechanics problems which are described in part statistically, two general approaches are most frequently used: linearization of the problem about a reference trajectory, or the so-called "Monte Carlo" technique with its more precise dynamics. The former approach was chosen for this study since it is in general more economical,

and since it effects great simplification of the analysis as will be shown. The general technique is identical to that of reference 1 and others.

The principal assumptions made for this study were that the lunar gravitational field is spherically symmetric and that all velocity increments after cut-off of the ascent state are considered to be impulsive. These assumptions simplify the computational procedure without significantly altering the results.

The transition matrices used to extrapolate the initial covariance matrices for dispersions in LEM position and velocity and the associated covariance matrix of LEM uncertainties (errors in the estimation of the vehicle position and velocity) are developed in Appendix A. The following equations summarize the computations required.

Let $\delta \underline{x}(t) = \begin{Bmatrix} \delta \underline{r}(t) \\ \delta \underline{v}(t) \end{Bmatrix}$ be the

dispersions about the nominal trajectory, and

$$\underline{e}(t) = \begin{Bmatrix} \delta \hat{\underline{r}}(t) - \delta \underline{r}(t) \\ \delta \hat{\underline{v}}(t) - \delta \underline{v}(t) \end{Bmatrix}$$

be the uncertainties in the trajectory estimate (i.e., $\delta \hat{\underline{r}}(t)$ is the estimated position dispersion). The linearized statistics of the problem are described by the covariance matrices

$$X(t) = E\left\{ \delta \underline{x}(t) \delta \underline{x}(t)^T \right\}$$

$$C(t) = E\left\{ \underline{e}(t) \underline{e}(t)^T \right\}$$

The extrapolation of these matrices in time is accomplished by

$$X(t_1) = \Phi(t_1, t_0) X(t_0) \Phi(t_1, t_0)^T$$

$$C(t_1) = \Phi(t_1, t_0) C(t_0) \Phi(t_1, t_0)^T$$

where $\dot{\Phi}(t,t_0) = \begin{bmatrix} 0 & I_3 \\ G & 0 \end{bmatrix} \Phi(t,t_0); \quad \Phi(t_0,t_0) = I_6$

$$G = \frac{\mu}{|\underline{r}_{LEM}|^5}\left(3\,\underline{r}_{LEM}\underline{r}_{LEM}^T - |\underline{r}_{LEM}|^2 I_3\right)$$

and

$$\dot{\underline{r}}_{LEM} = \underline{v}_{LEM}$$

$$\dot{\underline{v}}_{LEM} = \frac{\mu}{|\underline{r}_{LEM}|^3}\underline{r}_{LEM}$$

$$\dot{\underline{r}}_{CSM} = \underline{v}_{CSM}$$

$$\dot{\underline{v}}_{CSM} = \frac{\mu}{|\underline{r}_{CSM}|^3}\underline{r}_{CSM}$$

Although analytical solutions exist for the LEM and CSM state equations, these were integrated along with the transition matrix Φ for computational convenience. The trajectory model and the technique for extrapolation of the covariance matrices along the reference trajectory are now established.

II. MEASUREMENT MODEL

The LEM computer uses the Kalman filter technique to process measurement information for estimation of the vehicle's position and velocity. This process is described in references 1 and 2. To implement this technique, the on-board system propagates a covariance matrix of the uncertainties starting from an appropriate initial estimate (which need not be precise). At each measurement, this covariance matrix is used to generate a complete new state estimate through the error correlations contained in the covariance. The measurement is simultaneously used to reduce the uncertainties in the covariance matrix. A major economy of the linearization approach to error analysis is observed in this measurement process, since the generation of the linearized statistical description of the dispersions, uncertainties and associated corrective

velocity requirement never requires an explicit estimate of the state. The mathematics of the filtering technique are developed in Appendix B, and the resulting equations for manipulating the covariance matrix of uncertainties at a measurement are:

$$C(t^+) = C(t^-) - \frac{1}{a} C(t^-) \underline{h}\, \underline{h}^T C(t^-)$$

$$a = \underline{h}\, C(t^-) \underline{h}^T + \overline{\alpha^2}$$

where t^-, t^+ refer to time before and after the incorporation of the measurement with respect to state errors, and $\overline{\alpha^2}$ is the calibrated variance of the instrument.

Implicit in this presentation is that all the instrument errors are treated as if they had zero mean. This treatment is made possible by the simple technique of adding the biases of the instruments to the quantities to be estimated and processing the measurements such that bias estimates are realized right along with the vehicle state estimates.

The assumptions made in this development are consistent with those made by MIT for the on-board mechanization. Since some of these assumptions should be examined in future studies, they are listed below.

(a) The position of the CSM is assumed to be precisely known to the LEM. This is a good assumption only if the LEM estimation errors are significantly larger than the CSM estimation errors, which is not true for the more precise measurement schemes treated herein. This assumption should not influence the instrument comparison, but will influence the absolute fuel requirement.

(b) Vector measurements (i.e., range, aximuth and elevation measured simultaneously) are treated as a sequence of scalars and are introduced one piece of information at a time into the estimation scheme. This is proper only if the errors in the vector measurement are not correlated from element to element, and is a reasonable simplification for this problem.

(c) The measurement biases are assumed constant. This assumption is good as long as the biases vary slowly with respect to the measurement rate. The most significant bias is generally platform drift, and this is slow compared to the measurement rate of the schemes investigated.

The computation implementation of the filter included models of the calibration error for the radar which matched the specification values for the various measurement schemes as closely as possible.

III. GUIDANCE MODEL

The primary guidance scheme for the LEM ascent as developed by MIT has two distinct operation modes for the midcourse phase and for the terminal rendezvous phase. For the purposes of this study, the midcourse phase was considered to be from cut-off of the ascent state to the point where the relative range between the LEM and CSM had decreased to 6 N.M. The terminal phase extended from this condition to a range of 250 ft. and a relative velocity of about 5 ft./sec. The astronaut could assume manual control for the docking maneuver at or prior to this point. In the discussion that follows, the midcourse phase is treated first and then the terminal rendezvous portion is discussed.

The midcourse guidance in the MIT scheme is achieved by calculating explicit velocity corrections based on solutions to Lambert's problem for a fixed time of transfer from an initial position to a target position prescribed in inertial space. During this phase, the LEM is actually guided to intercept the CSM at a specified time. Since the on-board guidance is based on estimated state variables, a criterion is introduced to insure that velocity corrections are made at points where the estimated information is of good quality relative to the required velocity increment and to limit the total number of corrections.

Since a linearized statistical representation of the dispersions is used, it is convenient to linearize the guidance as well. A very natural linearization of Lambert's problem is already frequently used as a space guidance technique. This method depends on developing a transition matrix about the reference trajectory to relate position and velocity deviations at a desired correction point to position deviations at the target point. Thus, the velocity increment required can be calculated as a linear function of the position and velocity deviations at an arbitrary point. The details of the development of this method are presented in Appendix C, including a simple technique for calculating the guidance transition matrix. It should be noted that since the representation of the dispersions consists of a covariance matrix, the velocity increment required can also be characterized as a covariance matrix of the variances and correlations of each of the inertial components of the corrective velocity increment. While this representation contains more information than a quasi-deterministic velocity increment generated by a Monte Carlo technique, it does not explicitly describe the fuel requirement. This can be seen immediately if one notes that each component of the corrective velocity has a zero mean, but the fuel requirement associated with each is necessarily non-zero since it deals only with the magnitude of the corrections. However, the RMS value provided by the trace of this matrix does provide a measure of performance useful for the comparisons desired in this study.

In addition to accounting for the guidance velocity corrections, it is also necessary to describe the dispersions and uncertainties caused by

the implementation and measurement errors during a correction. This material is developed in Appendix D. In summary, the following equations describe the midcourse guidance process.

Let $\Psi(t, t_f)$ be the transition matrix from the present time to the target point. Partition Ψ (in (3×3)'s) as follows:

$$\Psi = \begin{bmatrix} \Psi_1 & \Psi_2 \\ \Psi_3 & \Psi_4 \end{bmatrix}$$

Then

$$B = \Psi_2^{-1}\Psi_1 - I_3$$

$$D = B(X(t^-) - C(t^-))B^T$$

$$\delta u = \sqrt{TR\, B C(t^-) B^T}$$

$$\delta v = \sqrt{TR\, D}$$

If the ratio $\delta u / \delta v$ is less than some prescribed number, the correction is added and

$$X(t^+) = (I_6 + JB)(X(t^-) - C(t^-))(I_6 + JB)^T + C(t^-) + \Delta X_{IMPL}$$

$$J = \begin{Bmatrix} 0 \\ I_3 \end{Bmatrix}$$

$$C(t^+) = C(t^-) + \Delta C_{IMPL}$$

The implementation errors are described by:

$$\Delta X_{IMPL} = J\left(K_1 D + K_2 I_3\right) J^T$$

$$K_1 = \frac{\overline{\sigma^2}\left(1-\overline{\gamma^2}\right) - \overline{\gamma^2}}{\delta v^2}$$

$$K_2 = \overline{\gamma^2}\left(\delta v^2 + \overline{\sigma^2}\right)$$

Where $\overline{\sigma^2}$ is the variance in tail-off error and $\overline{\gamma^2}$ is the variance in pointing error. Similarly,

$$\Delta C_{IMPL} = J Q J^T$$

$$Q = Q\left(K_x, K_y, K_z, \xi_x, \xi_y, \xi_z, \delta v^2\right), \quad (3\times 3)$$

where the K's are accelerometer scale factor errors, the ξ's are angular misalinements of the platform and the δv^2 involves the diagonal elements of D. Q is detailed in Appendix D.

Finally, the velocity requirement measure for the midcourse phase is:

$$\Delta V_{RMS} = \sqrt{\left(1+K_1\right)\delta v^2 + K_2}$$

In programing the midcourse guidance, it was found that the precision of the optical tracker and sextant was such that the uncertainties were quickly reduced to the point where frequent corrections would be made to remove the dispersions in the previous correction. Accordingly, an additional criterion was added that the magnitude of the velocity correction must exceed some specified limit. Also, the constraint was added that no correction should be made before 600 seconds after cut-off of the ascent stage to avoid possible problems with the singularities in the Lambert's problem solution.

In the terminal rendezvous phase, MIT has suggested two techniques for implementing the rendezvous guidance (see reference 1). The technique chosen for this study is that which consists of forcing an equivalent

range-rate schedule at particular range check points. The schedule adopted is one most frequently used by MIT, consisting of:

Checkpoint	Range	Equivalent Range-Rate
1	30,400.ft	100.ft/sec
2	9,120.	20.
3	1,520.	5.

The technique as implemented consists of testing the range until a checkpoint is crossed, then using the equivalent range-rate to calculate a time until rendezvous:

$$t_{go} = \frac{R}{\dot{R}}$$

The position of the CSM at $t+t_{go}$ is predicted, and is used together with the LEM's present position and t_{go} to form Lambert's problem, enabling the guidance to solve explicitly for the required present velocity. This operation is repeated at each checkpoint, causing successive decreases in the relative velocity while closing the relative range, until the vehicle lies within a region where manual docking is initiated.

The problem at hand is to account for the effects of dispersions and uncertainties due to the navigation and implementation of corrections on the corrective velocity requirement. Accordingly, a linearized guidance technique analogous to that of the midcourse phase was used to determine the additional increment required to null the position dispersions at $t+t_{go}$. Implicit in this approach is the assumption that the position dispersions are unchanged during the velocity correction of the reference trajectory. This is consistent with the impulsive velocity change already assumed. In programing the problem, it was decided to use the linearization of Lambert's problem to determine the reference trajectory velocity changes as well as the velocity increment covariance matrices. This was done because the accuracy of Lambert's problem in a straightforward formulation tends to break down in the terminal rendezvous region, while the accuracy of the linearization increases with decreasing relative range. Further, the transition matrix to the target was generated about the (assumed) circular CSM orbit since an analytical solution for this problem is available and there is no loss in accuracy. The details of the guidance development for the terminal rendezvous phase are in Appendix C. The resulting equations are the same as the midcourse correction calculations, except that the source of Ψ is changed, and D is augmented as follows:

$$D = B(X(t^-) - C(t^-))B^T + \Delta V \Delta V^T$$

Where ΔV is the reference trajectory velocity change, S_u^2 need not be computed, and the measure of additional velocity requirement for the terminal corrections is:

$$\Delta V_{RMS} = \sqrt{(1+K_1)S_u^2 + K_2} - |\Delta V|$$

The program was constructed to sum the midcourse ΔV RMS, and then to give a final summed ΔV RMS at the end of the run. The RMS dispersions and uncertainties in position and velocity were also computed and printed at each integration step from the third terminal correction to the 250' termination range.

A limitation of this study is that only the case where the LEM is active was considered. Alteration of the work to handle the case where the CSM orbit was manipulated would require changing the computation of the transition matrix to the target and changing the range/range-rate schedule in the terminal state to one suitable for CSM thrusting, which is a straightforward extension.

IV. DESCRIPTION OF MEASUREMENT SCHEMES

This section will outline the characteristics of the various measurement schemes studied.

The radar considered in this investigation was used in the mode prescribed by previous studies at MIT. In the midcourse phase, where relative range varies slowly, the radar measured range-rate and the elevation and azimuth angles of the line of sight from an inertial reference. During the terminal phase, when range-rate varies slowly, the radar measured range and the elevation and azimuth angles. In both phases, this data is assumed available at a one minute interval. The values used for the standard deviations (S.D.) of the various calibrated errors and initial standard deviations of the biases are tabulated below.

Range/Range-Rate Errors

Range	Range S.D.	Range-Rate S.D.
400 n.m. - 5 n.m.	.0833%	.0833% ± .33 fps
5 n.m. - 50 ft.	.33% ± 6.7'	.33% ± .33 fps

Range/Range-Rate Biases

Initial Range S. D. in Bias = 100 ft
Initial Range-Rate S. D. in Bias = 5 fps

Angle Errors

Range	Angle S.D.
400 n.m.	1.67 millirad.
200 n.m.	1. millirad.
5 n.m.	1. millirad.
2 n.m.	2. millirad.
1 n.m.	3.67 millirad.
50 ft.	3.67 millirad.

Angle Biases

Initial Elevation S.D. in bias = 1.14 millirad
Initial azimuth S.D. in bias = 1.14 millirad

The discontinuity in the range/range-rate errors at 5 n.m. was absorbed by switching from the range-rate mode to the range mode at that relative range. The angle error was characterized by allowing the standard deviation listed to lie in a plane which has polar orientation about the line of sight described by an angle with uniform density over the interval $(0, \pi)$. The resulting calibration errors for the filter are developed in Appendix B. The variation of this error with range was simulated by assuming a piecewise linear variation between each of the listed check-points. The initial bias errors are chiefly a result of alinement errors for the inertial platform.

The optical tracker considered measures the azimuth and elevation angles from an inertial reference to a line of sight established by tracking reflected light or a beacon on the other vehicle. This data was also assumed to be available at a one minute interval. The characterization of the angular errors was handled in the same way as for the

radar, with a standard deviation in the angle of 0.1 millirad. and in the initial bias of 1.1 millirad. The only constraint on sighting with the tracker was a range limitation of 300 n.m. Under some lighting conditions, the instrument cannot maintain track, but these were not considered in this study.

The VHF-sextant is a combination of a range measurement by the onboard VHF equipment and measurements of the azimuth and elevation angles from an inertial reference to the line of sight by the CSM sextant. This data was used in two modes; VHF-sextant measurements during midcourse and VHF ranging only during the terminal phase, and VHF sextant measurements during only the midcourse phase with an open terminal phase. In the open terminal phase, the state estimate is simply propagated with no additional measurements. The data is assumed to be available at two minute intervals for all modes. A 152 n.m. maximum range constraint was placed on the sextant, and 87 n.m. was the maximum for the VHF range. An additional constraint adopted for all schemes involving the sextant is that sextant measurements stop at a relative range of 15 n.m. This constraint arises from conflicting operational requirements which prevent the astronaut from making sightings beyond this point. The standard deviation used in range was 50 ft., and the initial standard deviation in bias was 100 ft. The sextant precision was assumed to be exactly the same as the optical tracker precision.

Finally, in the sextant configuration, the azimuth and elevation angles of the line of sight with respect to an inertial reference are assumed available at a two minute measurement interval during the midcourse phase only and subject to the same constraints as in the VHF-sextant case. To determine the effect of sighting rate on the problem, one and three minute measurement intervals were also run.

V. RESULTS AND DISCUSSION

A CDC 3600 digital computer program incorporating the trajectory and dispersion extrapolation, measurement and guidance techniques outlined in the previous sections was generated for this study. This program was used to calculate RMS corrective velocity requirement and RMS position and velocity dispersions and uncertainties in the neighborhood of manual takeover for docking (600 ft. range for the purpose of this study).

A single Hohmann transfer from 50,000 ft. to rendezvous with the CSM in an 80 n.m. circular orbit was studied. It has been shown (reference 3) that this type of transfer is applicable for aborts from the neighborhood of hover as well as for the direct ascent case. Initial covariance matrices corresponding to the following conditions were obtained from reference 4 and reference 1:

1. MIT direct ascent
2. PNGCS direct ascent
3. AGS direct ascent
4. PNGCS abort from hover
5. AGS abort from hover

Where PNGCS denotes that the primary navigations, guidance and control system has been used to steer the ascent boost, AGS denotes that the abort guidance system has been used, and MIT denotes that the initial covariance matrix used in most MIT studies has been assumed. The covariance matrices of reference 4 represent the results of an error analysis of the ascent thrusting with a hardware model based on current specifications. The MIT direct ascent covariance (reference 1) was included to allow comparisons with MIT results. For this problem it was assumed that the initial covariance matrices of uncertainties and dispersions were identical.

A list of the system errors effective during velocity corrections is included as table I. These errors were held constant throughout the investigation.

A preliminary study was made to optimize the choice of the criteria previously described for permitting midcourse corrections; the ratio of RMS velocity uncertainty to RMS velocity correction increment and the deadband for minimum permissible RMS velocity correction. Initial covariances corresponding to the PNGCS and MIT direct ascent modes were used in this work. These two initial covariance matrices of dispersions provide a good contrast, since the PNGCS case has a high degree of correlation and the MIT case has relatively little correlation. Results are presented in table II for the radar, the VHF-sextant with open terminal phase, and for the optical tracker. The VHF-sextant with VHF terminal phase and the sextant alone behaved in the same way as the VHF-sextant with open terminal phase.

The radar results are presented in table IIa. Since the deadband had little influence on the radar performance (all corrections tended to be large), the deadband was fixed at 3 fps and ratios of .1, .2, .3, .4 were used. For the nominal case (PGNCS) a ratio of .3 was best, while MIT initial covariance gave a minimum at .4. The ratio for the radar was set at .3 for further studies. Both ratio and deadband were varied for the VHF-sextant case. Ratios of .1, .2, .3 and .4 were used. and deadbands of 1., 2., 3. and 4. fps. These results are in table IIb. A comparison of the nominal and MIT covariance results gives a mutual best choice of ratio of .2 with a deadband of 2. fps, and these values were used for further work. Again, both ratio and deadband were varied for the optical tracker, with ratios of .1, .2 and .3 and deadbands of 1., 2. and 3. fps tested. These results are in table IIc. Consideration of both nominal and MIT results led to the choice of a ratio of .2 and deadband of 2. fps as the best compromise for further work. A general conclusion to be noted in the results for these three instrument schemes is that the fuel consumption is not strongly influenced by small variations in the ratio and deadband parameters.

Finally, with the error models previously described. all the measurement schemes were run for the complete spectrum of initial covariance matrices and for one standard deviation throughout. To help ascertain the sensitivity of the RMS corrective velocity increment, dispersions and

uncertainties to instrument inaccuracies, two standard deviations in the line of sight angular error for the radar was used with the remaining system errors held at one S.D., and similar cases were computed for a ten S.D. line of sight angular error for the remainder of the measuring schemes. In addition, some manipulation of the measurement rate (as described in section IV) was done.

The results of these runs appear in table III. The major conclusion to be drawn from these results is that the .1 millirad.S.D. in angular error for the optical tracker and sextant combinations gives these modes a decided advantage over the 1 millirad (plus) S. D. angular error of the radar. Over all cases in nominal modes, the optical tracker performs best, followed closely by the VHF-sextant and the sextant. The radar performance is somewhat poorer. The range or range-rate radar information at the specified precision does not appear to be particularly valuable compared to the angular information. During the latter stages of terminal rendezvous, however, this information helps reduce the uncertainties to very low levels. The very good precision of the VHF ranging near its maximum range is helpful for early midcourse corrections, but is not sufficiently potent to allow the combination to overshadow the optical tracker when the VHF-sextant is used at its slower operational measurement rate.

A side point is the effectiveness of bias estimation in making the high angular accuracy instruments useful. All these schemes are subject to the rather large uncertainty in platform alinement. The ability to estimate this type of error directly reduces the error which must be charged against the measuring scheme from the RSS of expected platform errors and calibration errors to the calibration error alone. A portion of the bias error is still charged against the scheme, since the variance in bias error is accounted for, but repeated measurements reduce the cost of this error considerably.

It should be noted that the early measurement accuracy of the sextant combinations is so good that even after running through the complete terminal phase with no additional measurements, the deviations and uncertainties in the docking region present no problems. Since manual takeover can certainly be initiated much sooner than the 600 ft. range considered here, this indicates a margin of safety for adverse lighting conditions, dropped measurements and the like.

Finally, even reduction of the angular precision of the optical tracker and sextant combinations from a .1 millirad. S.D. to a 1. millirad. S.D. does not significantly increase the measure of corrective velocity required, although the associated dispersions and uncertainties in the docking region are considerably degraded.

VI. CONCLUDING REMARKS

This paper reports the results of a linearized statistical error analysis of the Apollo Lunar Excursion Module Ascent and Rendezvous, including the guidance and navigation. The purpose of the study is to evaluate the radar measuring scheme,,and the following alternate schemes; an optical tracker, A VHF-sextant combination, and a sextant alone. A measure of the midcourse and terminal corrective velocity increment required by dispersions, and the RMS dispersions and uncertainties in position and velocity are generated to compare the efficiency of these measurement schemes.

The results indicate that the optical tracker is the most efficient sensor, followed closely by the VHF sextant and sextant alone, with the radar somewhat less efficient. This is to be expected, since the standard deviation of the angular error for the optical tracker and sextant is .1 millirad., whereas the radar angular accuracy is greater than or equal to 1 millirad.

The principal assumption included in this study that should be removed in future work is considering the CSM state to be precisely known for the LEM navigation. In particular, the accuracy of the optical tracker and the sextant combination sensors may make this assumption break down. A second area that requires more investigation is the explicit generation of the mean and variance of the velocity increments required by the dispersions, such that a quantitative measure of the fuel requirement is derived. Additional areas that bear investigation are extension to a more detailed dynamic model and inclusion of a more detailed error analysis of the steering during corrections. These considerations are not significant for the type of comparison desired in the problem at hand, but may have an effect on strict fuel consumption calculations.

List of Symbols

a	Weighting factor in filter
B	Guidance correction matrix (3 x 6)
C	Covariance matrix of uncertainties (6 x 6) or (9 x 9)
D	Covariance matrix of correction velocity increment (3 x 3)
e	Error in state estimate
G	Gradient matrix for transition matrix partition
$\underline{h}$	Measurement gradient vector
I_n	Unit matrix (n x n)
J	Coupling Matrix
$K_{1,2}$	Coefficients
$K_{x,y,z}$	Accelerometer scale factor error variances
Q	Velocity measurement error matrix
R	LEM-CSM relative range
$\dot{R}$	Relative range-rate
$\underline{r}$	Radius vector
t	Time
t_f	Time at rendezvous
t_{go}	Time until rendezvous
t^+, t^-	Time before and after a measurement incorporation
$\underline{V}$	Velocity Vector
$\underline{X}$	State Vector
X	Covariance matrix of dispersions

$\overline{\alpha^2}$	Calibrated variance in measurement angular error
$\overline{\gamma^2}$	Variance in angular error of velocity application
$\delta_{\underline{r}}$	Linearized position deviation
δ_u	RMS uncertainty in velocity
δ_v	RMS velocity requirement
$\delta_{\underline{V}}$	Linearized velocity deviation
$\delta_{\underline{X}}$	Linearized state deviation
$\delta\beta$	Linearized measurement deviation
ΔC_{impl}	Covariance partition of correction implementation uncertainties
$\Delta\underline{V}$	Reference trajectory velocity increment vector
ΔV_{RMS}	Measure of corrective velocity required by dispersions
ΔX_{impl}	Covariance partition of correction
μ	Lunar gravitational constant
$\xi_{x,y,z}$	Variances in platform angular misalinements
$\overline{\sigma^2}$	Variance in tail-off error
$\Phi(t_1, t_o)$	Transition matrix from time t_o to t_1
$\Psi(t_f, t_1)$	Transition matrix (for guidance) from time t_1 to t_f.

Subscripts

$(\ )_{CSM}$	CSM associated quantity
$(\ )_{LEM}$	LEM associated quantity

Operators

E	Mathematical expectation
$(\ )^T$	Matrix transpose
$(\underline{\ })$	Vector
$(\dot{\ })$	Differentiation with respect to time
$TR(\ )$	Trace of a matrix
$\lvert\ \rvert$	Magnitude of a vector
$\hat{(\ )}$	Denotes estimated quantity

TABLE I - SYSTEM ERRORS

1. S.D. of error in platform angular alinement, $\xi_x = \xi_y = \xi_z = 1.5$ millirad.

2. S.D. of error in accelerometer scale factor, $K_x = K_y = K_z = 6.33 \times 10^{-4}$.

3. S.D. of thrust tail-off error, $\sqrt{\overline{\sigma^2}} = .5$ fps.

4. S.D. of thrust dynamic misalinement error, $\sqrt{\overline{\delta^2}} = 1.73$ millirad.

UNCLASSIFIED

TABLE II. MIDCOURSE CORRECTION CRITERIA STUDY

a.) Radar Ratio Variation
Deadband = 3 ft./sec.
1 Standard Deviation Errors

COVARIANCE	RATIO	NO. CORRECTIONS	RMS $\sum \Delta V$ MID	RMS $\sum \Delta V$ TOT
PGNCS	.1	1	20.27	40.36
"	.2	2	21.80	30.19
"	.3	3	23.71	28.51
"	.4	4	24.93	29.14
MIT	.1	1	23.51	54.86
"	.2	2	25.85	37.60
"	.3	3	28.16	34.33
"	.4	4	28.48	33.55

b.) VHF - Sextant, Open Terminal Phase,
Ratio and Deadband Variations
1 Standard Deviation Errors
1. PGNCS Initial Covariance Matrix

RATIO	DEADBAND	NO. CORRECTIONS	RMS $\sum \Delta V$ MID	RMS $\sum \Delta V$ TOT
.1	1	2	16.45	19.09
"	2	2	16.45	19.09
"	3	2	16.97	19.22
.2	1	4	17.79	19.45
"	2	3	17.41	19.22
"	3	2	15.34	22.44
.3	1	5	19.03	20.72
"	2	3	17.40	20.83
"	3	3	18.35	20.62
"	4	3	19.54	21.33

UNCLASSIFIED

2. MIT INITIAL COVARIANCE MATRIX

RATIO	DEADBAND	NO. CORRECTIONS	RMS V MID	RMS V TOT
.1	1	2	20.65	23.83
	2	2	20.65	23.83
	3	2	21.01	23.79
.2	1	4	21.03	22.70
	2	3	20.58	22.54
	3	2	18.44	26.76
	4	2	18.92	25.59
.3	1	4	21.13	23.76
	2	3	20.10	25.34
	3	3	21.06	23.89
	4	3	22.20	24.20
.4	3	3	21.62	26.78
	4	2	18.92	25.59

UNCLASSIFIED

TABLE II. MIDCOURSE CORRECTION CRITERIA STUDY

c.) Optical Tracker Ratio
and Deadband Variations.

1. PGNCS Initial Covariance Matrix

RATIO	DEADBAND	NO. CORRECTIONS	RMS $\Sigma \vec{\Delta V}$ MID	RMS $\Sigma \vec{\Delta V}$ TOT
.1	1	2	15.90	18.12
"	2	2	15.90	18.12
"	3	2	15.90	18.12
.2	1	3	15.88	18.18
"	2	3	16.15	18.12
"	3	2	14.16	21.27
.3	1	4	16.56	18.56
"	2	3	15.66	18.46
"	3	2	14.16	21.27

2. MIT Initial Covariance Matrix

RATIO	DEADBAND	NO. CORRECTIONS	RMS $\Sigma \vec{\Delta V}$ MID	RMS $\Sigma \vec{\Delta V}$ TOT
.1	1	2	19.30	21.67
"	2	2	19.30	21.67
"	3	2	19.30	21.67
.2	1	3	18.80	21.00
"	2	3	18.80	21.00
"	3	2	16.67	25.21
.3	1	4	19.25	21.00
"	2	3	18.08	21.14
"	3	2	16.29	25.52

UNCLASSIFIED

TABLE III. PERFORMANCE OF MEASUREMENT SCHEMES FOR VARIOUS INITIAL COVARIANCE MATRICES

a.) Radar Performance
Ratio = .3 Deadband = 3.

RMS Dispersions and Uncertainties @ R = 715'.

1. 1 Standard Deviation Errors

Covariance	Mode	Number Corrections	RMS $\Sigma \Delta V$ Mid	RMS $\Sigma \Delta V$ Tot	RMS Dispersions ΔR	ΔV	RMS Uncertainties ΔR	ΔV
MIT	D.A.	3	28.16	34.33	165.	1.00	69.	.02
PGNCS	D.A.	3	23.71	28.51	163.	.98	69.	.02
PGNCS	A.B.H.	3	43.47	56.53	215.	1.40	70.	.02
AGS	D.A.	2	17.87	30.84	194	1.23	69.	.02
AGS	ABH	3	51.62	65.72	260.	1.73	70.	.02

2. 1 Standard Deviation Errors Except 2 Standard Deviation Line of Sight Angular Error

Covariance	Mode	Number Corrections	RMS $\Sigma \Delta V$ Mid	RMS $\Sigma \Delta V$ Tot	RMS Dispersions ΔR	ΔV	RMS Uncertainties ΔR	ΔV
MIT	D.A.	3	32.09	37.84	173.	1.03	81.	.03
PGNCS	D.A.	3	26.52	31.48	171.	1.01	81.	.03
PGNCS	A.B.H.	3	47.63	61.14	222.	1.42	81.	.03
AGS	P.A.	2	19.10	31.84	199.	1.24	81.	.03
AGS	A.B.H.	3	54.87	69.17	265.	1.75	81.	.03

D.A. Denotes Direct Ascent
A.B.H. Denotes Abort from Hover

UNCLASSIFIED

TABLE III. PERFORMANCE OF MEASUREMENT SCHEMES FOR VARIOUS INITIAL COVARIANCE MATRICES

b.) V.H.F. Sextant - V.H.F. Terminal
Ratio - .2 Deadband = 2.

RMS Dispersions and Uncertainties at Range = 611'.

1. 1 Standard Deviation Errors

Covariance	Mode	No. Corrections	RMS $\sum \Delta V$ Mid	RMS $\sum \Delta V$ Tot	RMS Dispersions ΔR	ΔV	RMS Uncertainties ΔR	ΔV
MIT	D.A.	3	20.58	22.57	161.	.95	102.	.20
PGNCS	D.A.	3	17.41	19.26	161.	.95	102.	.20
PGNCS	A.B.H.	3	37.68	42.79	194.	1.30	103.	.20
AGS	D.A.	3	18.13	20.99	175.	1.10	102.	.20
AGS	A.B.H.	3	46.24	56.47	234.	1.68	104.	.20

2. 1 Standard Deviation Errors Except 10 Standard Deviation Line of Sight Angular Error.

Covariance	Mode	No. Corrections	RMS $\sum \Delta V$ Mid	RMS $\sum \Delta V$ Tot	RMS Dispersions ΔR	ΔV	RMS Uncertainties ΔR	ΔV
MIT	D.A.	2	22.28	27.54	376.	1.09	346.	.39
PGNCS	D.A.	2	16.96	20.27	354.	1.05	324.	.36
PGNCS	A.B.H.	3	46.01	52.20	387.	1.45	339.	.38
AGS	D.A.	2	17.21	23.04	360.	1.18	324.	.36
AGS	A.B.H.	3	48.71	57.24	403.	1.73	339.	.38

D.A. Denotes Direct Ascent
A.B.H. Denotes Abort from Hover

UNCLASSIFIED

TABLE III. PERFORMANCE OF MEASUREMENT SCHEMES FOR VARIOUS INITIAL COVARIANCE MATRICES

c.) V.H.F. Sextant - Open Terminal
Ratio = .2 Deadband = 2.

RMS Dispersions and Uncertainties @ 611'.

1. 1 Standard Deviation Errors

Covariance	Mode	Number Corrections	RMS $\Sigma\Delta V$ Mid	RMS $\Sigma\Delta V$ Tot	RMS Dispersions ΔR	RMS Dispersions ΔV	RMS Uncertainties ΔR	RMS Uncertainties ΔV
MIT	D.A.	3	20.58	22.54	266.	.96	236.	.26
PGNCS	D.A.	3	17.41	19.22	266.	.96	235.	.26
PGNCS	A.B.H.	3	37.68	42.77	288.	1.31	236.	.26
AGS	D.A.	3	18.13	20.95	274.	1.11	235.	.26
AGS	A.B.H.	3	46.24	56.45	316.	1.69	237.	.27

2. 1 Standard Deviation Errors Except 10 Standard Deviation Line of Sight Angular Error

Covariance	Mode	Number Corrections	RMS $\Sigma\Delta V$ Mid	RMS $\Sigma\Delta V$ Tot	RMS Dispersions ΔR	RMS Dispersions ΔV	RMS Uncertainties ΔR	RMS Uncertainties ΔV
MIT	D.A.	2	22.28	27.50	459.	1.07	440.	.43
PGNCS	D A.	2	16.96	20.22	442.	1.03	424.	.40
PGNCS	A.B.H.	3	46.01	52.15	469.	1.44	435.	.42
AGS	D.A.	2	17.21	23.00	448.	1.17	424.	.41
AGS	A.B.H.	3	48.71	57.20	483.	1.72	435.	.42

D.A. Denotes Direct Ascent
A.B.H. Denotes Abort from Hover

UNCLASSIFIED

TABLE III. PERFORMANCE OF MEASUREMENT SCHEMES FOR VARIOUS INITIAL COVARIANCE MATRICES

d.) Sextant - Open Terminal
2 min. Interval

RMS Dispersions and Uncertainties @
R = 611'.

1. 1 Standard Deviation Errors.

Covariance	Mode	Number Corrections	RMS $\sum \Delta V$ Mid	RMS $\sum \Delta V$ Tot	RMS Dispersions ΔR	ΔV	RMS Uncertainties ΔR	ΔV
MIT	D.A.	3	21.94	23.97	463.	1.01	446.	.40
PGNCS	D.A.	3	18.00	19.95	405.	.99	386.	.36
PGNCS	A.B.H.	3	38.89	44.06	455.	1.34	425.	.39
AGS	D.A.	3	18.69	21.64	410.	1.13	385.	.36
AGS	A.B.H.	3	48.38	56.75	475.	1.70	428.	.39

2. 1 Standard Deviation Errors Except 10 Standard Deviation Line of Sight Angular Error.

Covariance	Mode	Number Corrections	RMS $\sum \Delta V$ Mid	RMS $\sum \Delta V$ Tot	RMS Dispersions ΔR	ΔV	RMS Uncertainties ΔR	ΔV
MIT	D.A.	2	36.37	39.56	340.	3.01	340.	2.79
PGNCS	D.A.	1	17.50	62.51	340.	3.40	340.	2.78
PGNCS	A.B.H.	2	53.30	83.44	341.	3.30	339.	2.79
AGS	D.A.	1	12.91	58.30	327.	3.37	326.	2.70
AGS	A.B.H.	2	62.53	88.40	339.	3.42	338.	2.78

D. A. Denotes Direct Ascent
A.B.H. Denotes Abort from Hover

UNCLASSIFIED

TABLE III. PERFORMANCE OF MEASUREMENT SCHEMES FOR VARIOUS INITIAL COVARIANCE MATRICES

e.) Sextant - Open Terminal Sighting Frequency Comparison
Ratio = .2, Deadband = 2 RPS.

RMS Dispersions and Uncertainties at a range of 611'.

Covariance	Mode	Mins/ Site	Number Corrections	RMS $\sum \Delta V_{Mid}$	RMS $\sum \Delta V_{Tot}$	RMS Dispersions ΔR	RMS Dispersions ΔV	RMS Uncertainties ΔR	RMS Uncertainties ΔV
PGNCS	D.A.	1	3	16.96	19.02	282.	.96	253.	.27
PGNCS	D.A.	2	3	18.00	19.95	405.	.99	386.	.36
PGNCS	D.A.	3	3	18.02	19.77	544.	1.04	530.	.47
AGS	A.B.H.	1	3	45.43	53.92	366.	1.69	301.	.31
AGS	A.B.H.	2	3	48.38	56.75	475.	1.70	428.	.39
AGS	A.B.H.	3	3	46.64	55.04	611.	1.73	575.	.51

D.A. Denotes Direct Ascent
A.B.H. Denotes Abort from Hover

TABLE III. PERFORMANCE OF MEASUREMENT SCHEMES FOR VARIOUS INITIAL COVARIANCE MATRICES

f.) Optical Tracker Performance

Ratio = .2, Deadband = 2.

RMS Dispersions and Uncertainties at Range = 611'.

1. 1 Standard Deviation Errors

Covariance	Mode	Number Corrections	RMS V Mid	RMS VTot	RMS Dispersions R	RMS Dispersions V	RMS Uncertainties R	RMS Uncertainties V
MIT	D.A.	3	18.80	21.00	137.	.95	35.	.07
PGNCS	D.A.	3	16.15	18.12	133.	.96	29.	.05
PGNCS	A.B.H.	4	37.12	41.27	173.	1.30	32.	.06
AGS	D.A.	3	17.51	20.34	148.	1.10	29.	.05
AGS	A.B.H.	3	44.45	52.59	216.	1.67	39.	.08

2. 1 Standard Deviation Errors Except 10 Standard Deviation Line of Sight Angular Error

Covariance	Mode	Number	RMS V Mid	RMS V Tot	RMS Dispersions R	RMS Dispersions V	RMS Uncertainties R	RMS Uncertainties V
MIT	D.A.	3	36.10	38.63	218.	1.12	117.	.18
PGNCS]	D.A.	3	30.14	32.36	200.	1.08	106.	.08
PGNCS	A.B.H.	4	55.44	60.23	232.	1.39	112.	.15
AGS	D.A.	3	27.36	30.36	209.	1.19	106.	.08
AGS	A.B.H.	3	57.20	66.37	264.	1.73	113.	.16

UNCLASSIFIED

APPENDIX A - TRANSITION MATRIX DEVELOPMENT

This appendix develops the linearized equations of motion and the associated transition matrix. Propagation of the covariance matrices by means of the transition matrix is also described.

Consider the dynamic equations of the state of the vehicle for a simple inverse square central force field;

$$\dot{\underline{r}} = \underline{v}$$
$$\dot{\underline{v}} = -\mu \underline{r} r^{-3} \quad , \quad r = |\underline{r}|$$

If these variables are regarded as reference quantities and are perturbed, the perturbation equations (to first order) are;

$$\delta\dot{\underline{r}} = \delta\underline{v}$$
$$\delta\dot{\underline{v}} = \mu r^{-5}\left(3\underline{r}\,\underline{r}^T - r^2\right)\delta\underline{r}$$

If a perturbation state is defined as

$$\delta\underline{x} = \begin{Bmatrix} \delta\underline{r} \\ \delta\underline{v} \end{Bmatrix}$$

the following simple representation for the linear perturbation equations results;

$$\delta\dot{\underline{x}} = F\,\delta\underline{x}$$

where

$$F = \begin{bmatrix} 0 & I_3 \\ G & 0 \end{bmatrix} \qquad G = \mu r^{-5}\left(3\underline{r}\,\underline{r}^T - r^2 I_3\right)$$

Consider the matrix differential equation

$$\dot{\Phi}(t,t_0) = F\Phi(t,t_0) \quad , \qquad \Phi(t_0,t_0) = I_6$$

The assertion is made that

$$\delta\underline{x}(t) = \Phi(t,t_0)\,\delta\underline{x}(t_0)$$

Which can be verified directly, since

$$\begin{aligned}\delta\dot{\underline{x}}(t) &= \dot{\Phi}(t,t_0)\,\delta\underline{x}(t_0) \\ &= F\Phi(t,t_0)\,\delta\underline{x}(t_0) \\ &= F\,\delta\underline{x}(t)\end{aligned}$$

The initial condition is

$$\delta\underline{x}(t_o) = \Phi(t_o, t_o)\,\delta\underline{x}(t_o) = \delta\underline{x}(t_o)$$

and since the solution of a linear differential equation of this type for given initial conditions is unique, the asserted equation must be the solution. The matrix $\Phi(t, t_o)$ is called the state transition matrix, since it provides a transition of the state from time t_o to time t.

Now consider the definition of the covariance matrix of dispersions:

$$X(t) = E\left\{\delta\underline{x}(t)\,\delta\underline{x}(t)^T\right\}$$
$$= E\left\{\Phi(t,t_o)\,\delta\underline{x}(t_o)\,\delta\underline{x}(t_o)^T\,\Phi(t,t_o)^T\right\}$$

and since $\Phi(t,t_o)$ is deterministic,

$$X(t) = \Phi(t,t_o)\,E\left\{\delta\underline{x}(t_o)\,\delta\underline{x}(t_o)^T\right\}\Phi(t,t_o)^T$$
$$= \Phi(t,t_o)\,X(t_o)\,\Phi(t,t_o)^T$$

If it is observed that the uncertainty $\underline{e}(t)$ is a perturbation of the state just as the dispersion vector $\delta\underline{x}(t)$, and hence obeys the same differential equation, it follows that

$$C(t) = E\left\{\underline{e}(t)\,\underline{e}(t)^T\right\}$$
$$= \Phi(t,t_o)\,C(t_o)\,\Phi(t,t_o)^T$$

Summarizing these developments:

$$\dot{\Phi}(t,t_o) = F\,\Phi(t,t_o)\,,\quad \Phi(t_o,t_o) = I_o$$

$$X(t) = \Phi(t,t_o)\,X(t_o)\,\Phi(t,t_o)^T$$

$$C(t) = \Phi(t,t_o)\,C(t_o)\,\Phi(t,t_o)^T$$

These are the equations required for extrapolation of the errors.

APPENDIX B

Kalman Filter Application

In this appendix, the equation for the optimal linear filter devised by Kalman and the linearized models corresponding to the various measurement schemes are developed. The treatment of the angular error calibrations for weighting the measurements is also described.

The navigation filter for a space mission is required to solve the following problem; having some initial estimate of the state and of the initial variances and correlations of the errors in the state and given a measurement corrupted by random noise and with fewer independent pieces of information then there are elements in the state to be estimated, then how can this measurement be used to give the greatest improvement (in some sense) in the state estimate. Typically, minimization of the sum of the squares of the errors in the estimate is the performance criterion. In reference 2, Kalman has devised a general solution to the linear problem.

In the LEM and CSM application, it is assumed that all measurements can be treated as sequences of scalars, i.e., that the errors in the various components of the measurement are uncorrelated. For this case, the solution to the filter problem is

$$\delta\hat{x}(t) = \Phi(t,t_0)\,\delta\hat{x}(t_0) + a^{-1} C(t) h \left[\delta\beta - h^T \Phi(t,t_0)\,\delta\hat{x}(t_0)\right]$$

$$a = h^T C(t) h + \sigma^2$$

$$C(t^+) = C(t) - a^{-1} C(t) h h^T C(t)$$

where $\delta\beta$ is the perturbation in the scalar measurement due to the dispersion δx, and to first order

$$\delta\beta = h^T \delta x + \alpha.$$

This result is stated without proof since the proof is available in reference 2 and elsewhere.

In the linearized error analysis, the only variables of interest are the covariance matrices of dispersions, estimated dispersions and uncertainties. A property of the Kalman filter is

$$E\{\delta\hat{x}\, e^T\} = 0$$

Using this property, the estimated dispersion matrix can be expressed directly as

$$\hat{X}(t) = X(t) - C(t)$$

Consequently, the only matrices which must be kept are X(t) and C(t), which can be done without resorting to computing the actual estimate.

In short, once the gradient vectors $\underline{h}$ for a particular measurement are defined, the effect of the measurement on the C matrix is known and no additional calculations are required.

Given the filtering scheme above, the next step is to develop the $\underline{h}$ matrix for the measurement schemes of interest. Rather than treating the particular hardware articles, general types of measurements will be considered and later combined as required. The axis system used is sketched below:

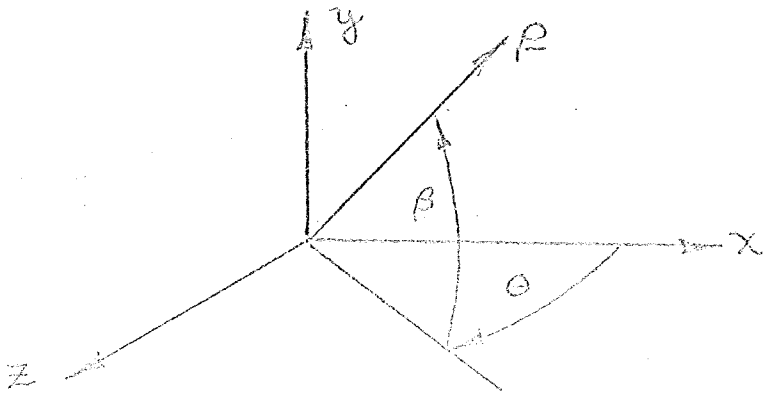

where ρ denotes the relative position vector between the CSM and LEM,

$$\rho = X_{CSM} - X_{LEM}$$

and

$$\delta\rho = -\delta X_{LEM}$$

The range measurement gradient vector is determined by:

$$R^2 = \rho^T\rho$$

$$\delta R = R^{-1}\rho^T\delta\rho + \delta R_{BIAS}$$

The range-rate measurement gradient vector is determined by:

$$\dot{R} = R^{-1}\rho^T\dot{\rho}$$

$$\delta\dot{R} = \left(\frac{\dot{\rho}^T}{R} - \frac{\dot{R}\rho^T}{R}\right)\delta\rho + \frac{\rho^T\delta\dot{\rho}}{R} + \delta\dot{R}_{BIAS}$$

The angle gradients are expedited by constructing $\underline{A}$, the projection of the $\underline{\rho}$ vector in the x-y plane

$$\underline{A} = M\underline{\rho} \qquad M = \begin{bmatrix} 1 & 0 & 0 \\ 0 & 0 & 0 \\ 0 & 0 & 1 \end{bmatrix}$$

and

$$\delta\underline{A} = M\,\delta\underline{\rho}$$

Then the elevation angle error gradient vector can be found by:

$$\cos\beta = \underline{\rho}^T \underline{A} \,/\, R|\underline{A}|$$

$$-\sin\beta\,\delta\beta = \frac{\underline{\rho}^T\delta\underline{A}}{R|\underline{A}|} + \frac{\underline{A}^T\delta\underline{\rho}}{R|\underline{A}|} - \frac{\underline{\rho}^T\underline{A}}{R^2|\underline{A}|}\delta R - \frac{\underline{\rho}^T\underline{A}}{R|\underline{A}|^2}\delta|\underline{A}|$$

$$|\underline{A}|^2 = \underline{\rho}^T M^T M \underline{\rho} = \underline{\rho}^T M \underline{\rho}$$

$$\delta|\underline{A}| = \frac{\underline{\rho}^T M\,\delta\underline{\rho}}{|\underline{A}|}$$

Substituting back, and with some additional manipulation,

$$\delta\beta = \frac{-1}{R\sin\beta}\left(\frac{\underline{A}^T}{|\underline{A}|} - \frac{|\underline{A}|\,\underline{\rho}^T}{R^2}\right)\delta\underline{\rho} + \delta\beta_{BIAS}$$

Then use the explicit representation of $\underline{\rho}$ and $\underline{A}$

$$\underline{\rho} = R\begin{Bmatrix} \cos\beta\cos\theta \\ \sin\beta \\ -\cos\beta\sin\theta \end{Bmatrix} \qquad \underline{A} = R\begin{Bmatrix} \cos\beta\cos\theta \\ 0 \\ -\cos\beta\sin\theta \end{Bmatrix}$$

$$|\underline{A}| = R\cos\beta$$

To find that

$$\delta\beta = \frac{1}{R}\begin{Bmatrix} -\sin\beta\cos\theta \\ \cos\beta \\ \sin\beta\sin\theta \end{Bmatrix}^T \delta\rho + \delta\beta_{BIAS}$$

For the azimuth angle error gradient, define

$$\underline{u}_x = N\underline{\rho} \qquad N = \begin{bmatrix} 1 & 0 & 0 \\ 0 & 0 & 0 \\ 0 & 0 & 0 \end{bmatrix}$$

Then

$$\cos\theta = \underline{u}_x^T \underline{A} \,/\, |\underline{A}|\,|\underline{u}_x|$$

$$-\sin\theta\,\delta\theta = \frac{\underline{u}_x^T \delta\underline{A}}{|\underline{A}|\,|\underline{u}_x|} + \frac{\underline{A}^T \delta\underline{u}_x}{|\underline{A}|\,|\underline{u}_x|} - \frac{\underline{u}_x^T \underline{A}\,\delta|\underline{A}|}{|\underline{A}|^2\,|\underline{u}_x|} - \frac{\underline{u}_x^T \underline{A}\,\delta|\underline{u}_x|}{|\underline{A}|\,|\underline{u}_x|}$$

and

$$|\underline{u}_x|^2 = \underline{\rho}^T N^T N \underline{\rho} = \underline{\rho}^T N \underline{\rho}$$

$$\delta|\underline{u}_x| = \frac{\underline{\rho}^T N \delta\underline{\rho}}{|\underline{u}_x|}$$

Making the appropriate substitutions as in the elevation case, where in addition

$$\underline{u}_x = R\begin{Bmatrix} \cos\beta\cos\theta \\ 0 \\ 0 \end{Bmatrix} \qquad |\underline{u}_x| = R\cos\beta\cos\theta$$

then

$$\delta\theta = \frac{-1}{R\cos\beta}\begin{Bmatrix} \sin\theta \\ 0 \\ \cos\theta \end{Bmatrix}^T \delta\rho + \delta\theta_{BIAS}$$

For the various measurement schemes considered, the $\underline{h}$ vector combinations for the information measured are drawn from the above list.

The error calibration for the angular error is handled in the following way. Consider the axis system above again,

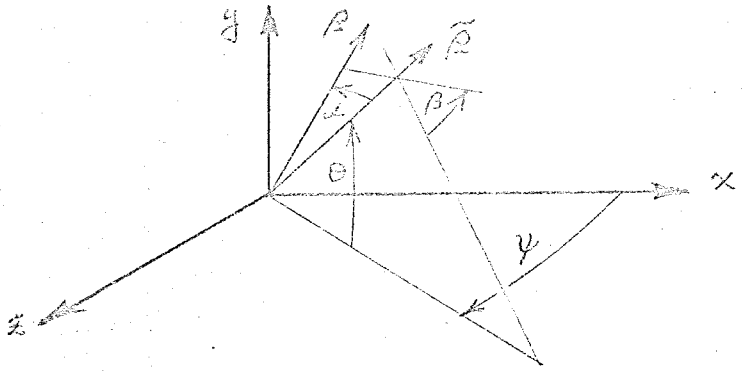

now, let α the the angular deviation due to instrument errors, and let it lie entirely in a plane whose polar orientation about the reference line of sight $\tilde{\rho}$ is defined by the angle β . Then, to first order,

$$\delta\theta = \alpha \cos\beta$$

$$\delta\psi = \alpha \sin\beta / \cos\theta$$

Assume that the angle α is a normally distributed random variable with zero mean, and that β is a random variable uniformly distributed over $(0, \pi)$. Then

$$\overline{\delta\theta^2} = \int_{-\infty}^{\infty}\int_{0}^{\pi} \alpha^2 \cos^2\beta \, p(\alpha)\, p(\beta)\, d\beta\, d\alpha$$

$$= \int_{-\infty}^{\infty} \alpha^2 p(\alpha)\, d\alpha \cdot \int_{0}^{\pi} \frac{\cos^2\beta\, d\beta}{\pi}$$

$$= \overline{\alpha^2}/2$$

where $\overline{\alpha^2}$ is the variance in α, and

$$\overline{\delta\psi^2} = \int_{-\infty}^{\infty}\int_{0}^{\pi} \frac{\alpha^2 \sin^2\beta}{\cos^2\theta}\, p(\alpha)\, p(\beta)\, d\beta\, d\alpha$$

$$= \overline{\alpha^2}/2\cos^2\theta$$

The cross-correlation is determined by

$$\overline{\delta\psi\,\delta\theta} = \int_{-\infty}^{\infty}\int_{0}^{\pi} \alpha^2 \sin\beta\cos\beta\, p(\alpha)\, p(\beta)\, d\beta\, d\alpha$$

$$= \int_{-\infty}^{\infty} \alpha^2 p(\alpha)\, d\alpha \cdot \frac{1}{\pi}\int_{0}^{\pi} \sin\beta\cos\beta\, d\beta$$

$$= 0$$

Since the errors in the assumed configuration are uncorrelated, the assumption that they can be treated successively as scalars holds. However, in the real case the characteristics of gimbals and output signal generators would probably cause a correlation to exist, and this effect should be checked when empirical calibration information becomes available.

APPENDIX C

Guidance Technique

This appendix treats this formulation of the midcourse guidance technique and the terminal guidance technique.

For the midcourse problem, the actual guidance system will use the solution to Lambert's problem for some reference target position and a reference transfer time. This fixed time, fixed target problem has a simple linearized equivalent using the transition matrix $\Psi(t_f,t)$ relating the state deviation at time t to the state deviation at t_f, with $\Psi(t_f,t)$ computed along the reference trajectory. Thus, the dispersion state can be propagated by:

$$\delta \underline{x}(t_f) = \Psi(t_f,t)\, \delta \underline{x}(t)$$

The desired end condition is

$$\delta \underline{r}(t_f) = \underline{0}$$

Hence, partitioning the Ψ matrix,

$$\begin{Bmatrix} \delta \underline{r}(t_f) \\ \delta \underline{v}(t_f) \end{Bmatrix} = \begin{bmatrix} \Psi_1 & \Psi_2 \\ \Psi_3 & \Psi_4 \end{bmatrix} \begin{Bmatrix} \delta \underline{r}(t) \\ \delta \underline{v}(t) \end{Bmatrix}$$

Leads to the required velocity,

$$\delta \underline{v}(t) = \Psi_2^{-1} \Psi_1\, \delta \underline{r}(t)$$

The change in velocity at a correction is the difference between the dispersion velocity prior to a correction and this required velocity, i.e.,

$$\begin{aligned} \Delta \underline{v}(t) &= \left[\Psi_2^{-1} \Psi_1 - I_3 \right] \delta \underline{x}(t) \\ &= B\, \delta \underline{x}(t) \end{aligned}$$

The quantity of interest in this investigation is the covariance matrix of the velocity correction,

which is calculated based on the best estimate of the dispersions. This is expressed by;

$$E\left\{\Delta\hat{\underline{V}}(t)\,\Delta\hat{\underline{V}}(t)^T\right\} = E\left\{B\,\delta\hat{x}(t)\,\delta\hat{x}(t)^T B^T\right\}$$
$$= B\,\hat{X}(t)\,B^T$$

But, as was seen in Appendix B,

$$\hat{X}(t) = X(t) - C(t)$$

Expressing the complete change of state,

$$X(t^+) = (I_6 + JB)\left[X(t^-) - C(t^-)\right](I_6 + JB)^T + C(t^-)$$

where

$$J = \begin{Bmatrix} 0 \\ I_3 \end{Bmatrix}$$

One additional consideration was an economical method of making the guidance transition matrix $\Psi(t_f, t)$ available at every time interval when it was desired to check for a correction. This was accomplished by obtaining the total transition matrix from the initial time to the target time, $\Psi(t_f, t_o)$, defining the differential equation for $\Psi(t_f, t)$ and integrating it numerically. The differential equation is obtained as follows:

$$\Psi(t_f, t_o) = \Psi(t_f, t)\,\Phi(t, t_o)$$

Hence

$$\dot{\Psi}(t_f, t_o) = 0 = \dot{\Psi}(t_f, t)\Phi(t, t_o) + \Psi(t_f, t)\dot{\Phi}(t, t_o)$$
$$= \dot{\Psi}(t_f, t)\Phi(t, t_o) + \Psi(t_f, t)F\Phi(t, t_o)$$

Therefore

$$\dot{\Psi}(t_f, t) = -\Psi(t_f, t)F$$

The terminal rendezvous guidance was accomplished by using an analytical solution for the transition matrix developed about the assumed circular CSM orbit. This solution is described in reference 5 for a different reference axis system. For the current investigation,

The required B matrix needs only the first two partitions of the $\Psi(t_f, t)$ matrix. These partitions are:

$$\Psi_1(t_f,t) = \begin{bmatrix} 1-c(1-c) & 0 & 2s(1-c)-3c(\Omega-s) \\ 0 & c & 0 \\ s(1-c) & 0 & 1+2c(1-c)+3(\Omega-s) \end{bmatrix}$$

$$\Psi_2(t_f,t) = \frac{1}{\mathring{\Omega}} \begin{bmatrix} s(2-c)-3c(\Omega-s) & 0 & -(1-c)(2-c)+3s(\Omega-s) \\ 0 & s & 0 \\ 1-c(2-c) & 0 & s(2-c) \end{bmatrix}$$

where

$$c = \cos\Omega \qquad s = \sin\Omega$$

$$\mathring{\Omega} = \sqrt{\mu / |\underline{r}_{csm}|^3}$$

$$\Omega = \mathring{\Omega}\, t_{go} \qquad t_{go} = R/\mathring{R}$$

This transition matrix is then used to compute the explicit velocity change on the reference trajectory, using the initial reference displacement of the LEM from the CSM and requiring that displacement to be nulled at $t = t + t_{go}$. Hence

$$\hat{\Delta \underline{V}} = B \begin{Bmatrix} \rho \\ \dot{\rho} \end{Bmatrix}$$

$$B = \left[\Psi_2 \Psi_1^{-1} - I_3 \right]$$

The same matrix is used to condition the dispersions in the same manner as for midcourse corrections.

APPENDIX D

Velocity Correction Implementation Errors

Two types of error inputs arise during a velocity correction, errors due to the dynamics of the control scheme and misalinements of the thruster, and errors due to inaccuracies in the inertial reference scheme. In this study the former errors were assumed to result from a net angular offset uncertainty and a thrust tailoff uncertainty. For the small velocity changes considered, those should be the principal error sources. Details of the development of this type of error are contained in reference 6. The resulting equation is:

$$\Delta X_{IMPL} = J(K_1 D + K_2 I_3) J^T$$

$$K_1 = \frac{\overline{\sigma^2}(1-\overline{\gamma^2})}{SV^2} - \overline{\gamma^2}$$

$$K_2 = \overline{\gamma^2}(SV^2 + \overline{\sigma^2})$$

where $\overline{\sigma^2}$ and $\overline{\gamma^2}$ are the variances of the thrust tailoff error and the pointing error, respectively.

In addition, the principal inertial reference errors, i.e., the angular alinement uncertainties and accelerometer scale factor error, were accounted for. The resulting error matrix is:

$$Q = \begin{bmatrix} \overline{K_x^2} SV_x^2 + \overline{\xi_y^2} SV_y^2 + \overline{\xi_z^2} SV_z^2 & -\overline{\xi_z^2} SV_x SV_y & -\overline{\xi_y^2} SV_z SV_x \\ -\overline{\xi_z^2} SV_x SV_y & \overline{K_y^2} SV_y^2 + \overline{\xi_x^2} SV_z^2 + \overline{\xi_z^2} SV_x^2 & -\overline{\xi_x^2} SV_z SV_y \\ -\overline{\xi_y^2} SV_x SV_z & -\overline{\xi_x^2} SV_y SV_z & \overline{K_z^2} SV_z^2 + \overline{\xi_x^2} SV_y^2 + \overline{\xi_y^2} SV_x^2 \end{bmatrix}$$

where $\overline{K^2}_{x,y,z}$ are the variances in the accelerometer scale factors and $\overline{\xi^2}_{x,y,z}$ are the variances in the platform misalinement angles.

REFERENCES

1. Apollo Report R-446, MIT Instrumentation Laboratory

2. Kalman, R. E., "A New Approach to Linear Filtering and Prediction Problems," Journal of Basic Engineering, March, 1960.

3. Gray, A. and Stull, P., "Study of LEM Abort Trajectories," MSC Internal Note No. 64-EG-20.

4. Kidd, R. H., and Henson, J.R., "Position and Velocity Error Covariance Matrices at Thrust Termination for the Apollo LEM," MSC Internal Note No. 65-EG-12.

5. Levine, G. M., "The Transition Matrix for a Circular Orbit," MIT Space Guidance Analysis Memo No. 11-64.

6. Carney, T. M., and Jones, E. M., "Preliminary Study of Benefits of Early Corrections and RCS Vernier Velocity Control for Apollo Midcourse Velocity," MSC Internal Note No. 64-EG-13.